

An Optimal Boundary Control of Thermal System with Experimental Verification

Tomáš Hruz¹

Boris Roháč-Iľkiv²

Zuzana Országhová³

Abstract

In this article an experimental verification of the step-wise control method containing an ill-posed problem solution as developed in [12] is presented. The controlled thermal system is considered to be decomposed into two subsystems - a subsystem which is easy to control by a feedback using measurable outputs of the system and a subsystem with a distributed state - usually a spatial temperature distribution inside a heated material - which is inaccessible to direct measurement. The dynamics of the state is supposed to be described by a suitable distributed parameter model with a boundary excitation performed via the measurable system output. The control task then consists of optimally varying the measurable system output that governs the boundary excitation of the distributed parameter subsystem until it is calculated that the required shape of the distributed state has been reached. In the article optimal reference values for the system output, which should be tracked by a controller, are generated using a stepwise technique for the inversion of the distributed parameter model. The experimental results justifying the proposed method and some numerical aspects of the method are also discussed.

Keywords: *Distributed parameter systems; inverse modelling; regularization; spline approximation; predictive control.*

1. Introduction

Heating of solid materials is one of the most energetically exhausting technological steps in heavy industry. Therefore the optimal heating is one of the research targets in control theory. Unfortunately the heating process is described by partial differential equations (distributed parameter system) and therefore it is not easy to transfer the well working theory from finite dimensional systems (ordinary differential equations) to this area. Moreover, most frequently the spatial temperature distribution inside the solid material during the heating is not accessible to direct measurement. Therefore, the problem is how to manipulate unmeasurable internal temperature distribution which can be only modelled by solving the infinite dimensional model equations. Although, recently a well developed theory of control for infinite dimensional systems has been proposed, as was noted for example in [4, 5] it is still a problem to realize such controllers

numerically.

The main reason for the numerical difficulties in the boundary control of thermal process inside a heated solid material stems from the ill-posedness of the model inversion which always is, in one way or other, embedded within the control algorithm [19].

In [12] the authors have proposed a control algorithm which clearly identifies the ill-posed part and splits the system into a pair of subsystems - a subsystem with measurable outputs (surface - boundary temperature of the heated object) which is easy to control by a feedback and a subsequent subsystem which is driven by the preceding subsystem and whose distributed state is inaccessible to direct measurement (inside temperature of heated object). Control of this inside temperature is achieved not by a feedback but by a maintaining of pre-calculated temperature time profile at the boundary of the object. The calculation of this boundary temperature time development is exactly the ill-posed part of the controller as was noted for example in [6].

The aim of this article is to submit an experimental verification of a method developed in [12] on laboratory system simulating a boundary heating. The method uses a predictive control system working with the measurable output of the thermal system and tracking a specified, optimally pre-calculated reference signal for boundary control of the system in order to obtain a required spatial temperature profile in the heated object at a selected time instants t_v . For a given spatial temperature profile, the reference signal for the system boundary control is obtained by inverting a distributed parameter model, which describes the dynamics of the unmeasurable temperature distribution in the second subsystem of the given thermal system. In the method the inverse problem is converted to some *regularization* problem and is solved by a *stepwise* technique. This technique seems to be suitable for on-line control of thermal systems under a condition of stochastic disturbances acting on the controlled systems. The dynamics of the first subsystem is modelled by continuous-time convolutional integrals with finite-support kernels. The input and output signals of the subsystem are considered to be polynomial splines. The B-splines are taken as base functions of these splines. The control synthesis is based on minimization of an integral continuous-time quadratic loss function, after the spline approximation is transformed to a simple matrix quadratic form. To minimize this form a quadratic programming is employed. The allowed control input signal is then defined by a set of suitably selected linear equality and inequality constraints which act on the vector of the polyno-

¹Slovak Technical University, Faculty of Mechanical Engineering, Department of Automatic Control and Measurement, Námestie Slobody 17, 812 31 Bratislava, Slovak Republic, Phone: +42-7-497193, 493041/ext.571 E-mail: hruz@vm.stuba.sk

²Same as above.

³MicroStep Ltd., Bratislava, Slovak Republic

mial coefficients of this signal.

In the following parts of the article we briefly mention the step-wise method developed in [12], inversion task and the overall algorithm. Then, certain discretization and numerical aspects of the method are described in more detail. At the end, the experimental device and its model are described together with the experimental results justifying the method. We conclude with some notes about possible work in future.

2. Step-wise method of optimal boundary control

The laboratory device which we describe later in more detail consists in a boundary heated metal bar which is cooled by heat transfer to the surrounding air. Then the behaviour of the unmeasured temperature field of the metal bar $s(x, t)$ at the time instant t and the position x of the bar is described by the parabolic partial differential equation:

$$\begin{aligned} \frac{\partial}{\partial t} s(x, t) - a^2 \frac{\partial^2}{\partial x^2} s(x, t) + bs(x, t) &= 0 \\ s(x, t_0) = s_0(x), s(0, t) = y(t), \frac{\partial s}{\partial x}(L, t) &= 0 \\ 0 \leq x \leq L, \quad t \geq t_0, \quad a \neq 0 \\ a^2 = \frac{\lambda}{c \cdot \rho}, \quad b = \frac{h}{c \cdot \rho} \end{aligned} \quad (1)$$

where: L is the length of the bar; λ is the thermal conductivity coefficient; c is the specific heat; ρ is the specific mass of the bar and h is the heat-transfer coefficient.

The Green's function $G(x, \xi, t)$ for the above problem is:

$$G(x, \xi, t) = \frac{2}{L} \sum_{n=0}^{\infty} \exp(-bt - \lambda_n t) \varphi_n(x) \varphi_n(\xi) \quad (2)$$

where $\varphi_n(x) = \sin \frac{\sqrt{\lambda_n} x}{a} = \sin \frac{(2k+1)\pi}{2L} x$ are eigenfunctions of the Sturm-Liouville problem for (1) with eigenvalues $\lambda_n = \frac{(2k+1)^2 \pi^2 a^2}{4L^2}$.

Then the solution of the equation (1) can be given in the following integral form:

$$s(x, t) = \int_{t_0}^t \int_0^L G(x, \xi, t - \tau) w(\xi, \tau) d\xi d\tau \quad (3)$$

where $w(x, t)$ is a *standardizing* function (see [2]):

$$w(x, t) = s_0(x) \delta(t) + a^2 \delta'(x) y(t) \quad (4)$$

which includes an exiting function, boundary and initial conditions and $\delta(\cdot)$ is the Dirac function. The heating of the bar is controlled through the boundary temperature $y(t) = s(0, t)$ and the task is to find such function $y(t)$ - boundary heating of the bar - which ensures the attainment of the required

spatial distribution of the bar temperature $s(x, t)$ at a specified time instant t_v . In this situation the relation (3) simplifies to the following form:

$$\begin{aligned} s(x, t_v) &= a^2 \int_{t_0}^{t_v} \frac{\partial}{\partial \xi} G(x, \xi, t_v - \tau) |_{\xi=0} y(\tau) d\tau + \\ &+ \int_0^L G(x, \xi, t_v - t_0) s_0(\xi) d\xi \end{aligned} \quad (5)$$

where $s_0(x) = s(x, t_0)$ is given initial condition. The second part of equation (5) is known for known initial conditions. Let us denote it as $s_c(x, t_v)$ and define the modified state $s_m(x, t_v)$ as:

$$s_m(x, t_v) = s(x, t_v) - s_c(x, t_v)$$

then

$$\begin{aligned} s_m(x, t_v) &= \\ &= a^2 \int_{t_0}^{t_v} \frac{\partial}{\partial \xi} G(x, \xi, t_v - \tau) |_{\xi=0} y(\tau) d\tau \end{aligned} \quad (6)$$

This equation can be written in an operator form:

$$s_m = Ay \quad s_m \in S, \quad y \in Y \subseteq Z \quad (7)$$

where A is the linear integral operator of relation (6), Z and S are Hilbert spaces, Y is a closed convex set, build by a priori limitations of the control task. The relation (7) represents an Fredholm integral equation of the first type and, the solution of this equation fulfils the definition of the *ill-posed problems* in the Hadamard's sense. Therefore it is necessary to use some *regularization* method, which will give satisfactory results. In this article we employ the method of Tikhonov [18], where the task of solving the equation (7) is replaced by the task of the minimization of the following *smoothing functional* $M_\alpha[y]$:

$$M_\alpha[y] = \| A_h y - s_m \delta \|^2 + \alpha \| y \|^2 \quad (8)$$

where $\alpha > 0$ is the regularization parameter.

A_h is an operator which approximates the operator A with defined error h , that means

$$\| A_h - A \| \leq h, \quad (9)$$

$s_m \delta$ is the left hand side of (7), which is specified by the error δ , i.e.

$$\| s_m - s_m \delta \| \leq \delta, \quad (10)$$

The so-called *generalized deviation* is defined as :

$$\begin{aligned} \rho(\alpha) &= \| A_h y_\alpha - s_m \delta \|^2 - \\ &- (\delta^2 + h \| y_\alpha \|^2) - (\mu(s_m \delta, A_h))^2 \end{aligned} \quad (11)$$

where

$$\mu(s_m \delta, A_h) = \inf_{y \in Y} \| A_h y - s_m \delta \|^2$$

is the *degree of inconsistency*.

The regularization parameter α of the smoothing functional is chosen by *generalized principle of deviation*, which is the following. If the condition:

$$\|s_{m\delta}\|^2 > \delta^2 + (\mu(s_{m\delta}, A_h))^2 \quad (12)$$

is not fulfilled, the approximate solution of the equation (7) is $y = 0$. If the condition (12) is fulfilled, then the generalized deviation (11) has a positive root α^* and the solution of equation (7) is a minimum y_{α^*} of the smoothing functional (8).

In [18] various properties of the generalized deviation has been proved. An important fact for our algorithm is that in the presence of constraints the generalized deviation is not a differentiable function of α and therefore the numerical method used can only employ the values of function $\rho(\alpha)$ in order to localize the root. However, the generalized deviation as a function of α is continuous, monotonic and therefore has only one zero.

As regards to the accuracy of the proposed procedure, the Tikhonov theory do not specify the precision to which a computation of the solution of equation $\rho(\alpha) = 0$ has to be carried out. However, in an experimental situation with noisy data few decadic places were enough.

2.1. Overall algorithm

In the preceding section the inverse task for the distributed model (1) was transformed to the problem of solving the operator equation (7) for a given left hand side. The solution $y_{\alpha^*} = y_r(t)$ of this equation forms the reference signal for the optimal boundary control of the heated bar. The iterative regularization method used for solving equation (7) is valid only for in advance given and constant integral bounds t_0, t_v . This fact is necessary to take into account in the designing of the generator of the reference signal $y_r(t)$ for on-line boundary control of the thermal system. One way is to base the generator structure on *stepwise triggering* the inversion task in equidistantly located discrete time instants t_v . The distance between the time instants determines the bounds of integrals in the numerical solution of the equation (7) and in next explanation we will call this distance the *inversion horizon* T_v . From a practical point of view the length of the horizon T_v depends on several factors, namely,

- Technological needs for the heating process and the goal of the heating.
- Dynamical properties of the thermal system.
- Time behaviour of disturbances acting on the measurable system output.

In the process of the stepwise triggering of the inversion task with the time period T_v it is necessary to know at the particular starting time instant a *true* profile of the unmeasurable temperature distribution $s(x, t)$ in the heated bar. The true profile $s(x, t)$, which is really reached at the end of a preceding period, creates the initial condition for the inversion in a subsequent period. Because the temperature profile $s(x, t)$ is not measured, its true time development can be only *simulated* using a response of the model (1) due to the actually measured system output signal $y(t)$. For numerical calculation of the true response $s(x, t)$, it is advantageous to utilize again the operator form (7) of

the model. The length of the time interval during which the integration in (7) with the real signal $y(t)$ is performed we will call a *simulation horizon* T_m . For numerical reasons it is suitable to choose $T_m = T_v/ni$, where ni is a given positive integer.

The starting point for the numerical solution of the simulation and the inversion tasks consists in a suitable discretization of the basic relation (7) and its transformation to a matrix form. The resulting matrix form oriented to the simulation we will call a *simulation* model and the matrix form aimed at the inversion we will call an *inversion* model. Based on the above models, the generator of the reference signal $y_r(t)$ is constructed. The required profiles $s_2(x)$ enter the generator with time period T_v and the real measured signal $y(t)$ enters the generator with period T_m .

3. Some numerical aspects of the proposed method

In this section we focus on two points. The first one is related to the robust computation of the integral kernels for boundary heated system which are derived from the Green's function. Another one is related to the numerical problems near to the heated boundary where the modelling with a Green's function needs a special provision to give reliable data.

3.1. Optimization of Green's function computation

As was noted in [17] (pp.218) the summation of the Fourier series is itself an ill-posed problem. Even if the ill-posedness is weaker than that of the heat conductivity inversion it is still good to know the reasons for the numerical problems which sometimes occur. During the computation of the Green's function it can be observed that slight changes in the algorithm, or bounds, lead to very different results.

In the case of the system described by equation (1), the solution (5) can be expressed with the following two integral kernels:

$$\frac{\partial}{\partial \xi} G(x, \xi, t) |_{\xi=0} = G_{\partial \xi}(x, t)$$

$$G(x, \xi, T) = G_T(x, \xi)$$

where

$$G_{\partial \xi}(x, t) = \frac{\pi}{L^2} \sum_{n=0}^{\infty} (2n+1) \exp(-bt - \lambda_n t) \varphi_n(x) \quad (13)$$

$$G_T(x, \xi) = \frac{2}{L} \sum_{n=0}^{\infty} \exp(-bT - \lambda_n T) \varphi_n(x) \varphi_n(\xi)$$

We propose an optimized method for the computation of the Green's function which contains accurate error bounds. The advantage of such a method can be seen when accurate results are needed near zero in time and near the heated boundary in space. In this case the points near time zero can easily require many thousands of terms in the series but as the time increases this number immediately drops to less than about 10.

We first turn our attention to the kernel $G_{\partial\xi}(x, t)$ and later it will be seen that the kernel $G_T(x, \xi)$ can be represented in a similar form.

The kernel $G_{\partial\xi}(x, t)$ can be written in the following form:

$$G_{\partial\xi}(x, t) = \frac{\pi}{L^2} \sum_{n=0}^{\infty} (2n+1)^2 \exp(-bt - \lambda_n t) \times \frac{\varphi_n(x)}{2n+1} \quad (14)$$

It is known from the basic theory of Fourier series that $\sum_{n=0}^{\infty} \frac{\varphi_n(x)}{2n+1} = \sum_{n=0}^{\infty} \frac{\sin(2n+1)\frac{\pi x}{2L}}{2n+1} = \pi/4$ when $0 < x < \pi$. Let us denote $M_n = (2n+1)^2 \exp(-bt - \lambda_n t)$. $M_n > 0$ is positive for all $n \geq 0$. M_n as a function of $n \geq 0$ has only one extremal point as follows from the properties of exponential function. This extremal point can be computed taking the derivative of M_n as a function of n , i.e.

$$\frac{d}{dn} ((2n+1)^2 \exp(-bt - \lambda_n t)) = 0$$

$$n_0 = \lceil (\frac{2L}{\pi a} \sqrt{\frac{1}{T}} - 1)/2 \rceil$$

Thus for all $n \geq n_0$ the sequence M_n is monotonically decreasing to zero.

We denote $S(k) = \sum_{n=0}^k \frac{\varphi_n(x)}{2n+1}$ the partial sum of $\sum_{n=0}^{\infty} \frac{\varphi_n(x)}{2n+1}$ and with $R(k) = \sum_{n=0}^{\infty} \frac{\varphi_n(x)}{2n+1} - S(k) = \sum_{n=k+1}^{\infty} \frac{\varphi_n(x)}{2n+1}$ the residual part of the series. Using the Dirichlet criterion we can conclude that

$$\left| \sum_{n=k+1}^{\infty} M_n \frac{\varphi_n(x)}{2n+1} \right| \leq M_{k+1} |R(k+1)| \quad (15)$$

or,

$$\left| \sum_{n=k+1}^{\infty} M_n \frac{\varphi_n(x)}{2n+1} \right| \leq M_{k+1} \left| \frac{\pi}{4} - S(k) \right|$$

whenever $k \geq n_0$. Thus the algorithm can compute the relative error of the series sum using the term $M_{k+1} \left| \frac{\pi}{4} - S(k) \right|$.

For the kernel $G_T(x, \xi)$, a similar method can be used by taking into account the following: the following:

$$\varphi_n(x)\varphi_n(\xi) = \frac{1}{2} \left[\cos \frac{(2k+1)\pi}{2L} (x - \xi) - \cos \frac{(2k+1)\pi}{2L} (x + \xi) \right]$$

$$\sum_{n=0}^{\infty} \frac{\cos(2n+1)\frac{\pi x}{2L}}{(2n+1)^2} = \frac{\pi x}{2L} - \frac{\pi}{2}$$

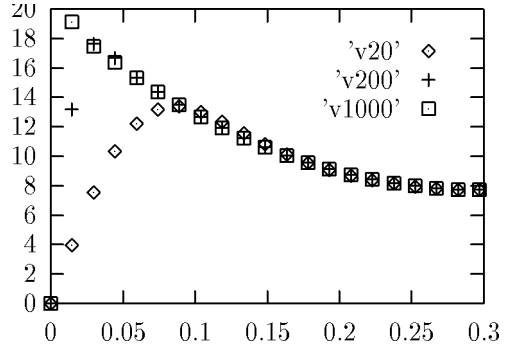


Figure 1: The numerical study of the relation between the space and time grids for the equation (16). The x-axis represents spatial coordinate in meters and the y-axis the temperature in degrees Celsius. The boundary condition was constant, namely $y(t) = 20$.

3.2. Accuracy of the simulation near the heated boundary

The major numerical problems encountered during the simulation and inversion in the method are related to the kernel $G_{\partial\xi}(x, t)$. Therefore, let us suppose for the simplicity that in (5) the initial condition $s_0(x)$ is zero. Then the state of the system in a certain time instant t can be written according to equation (5) as:

$$s(x, t) = a^2 \int_{t_0}^t G_{\partial\xi}(x, t - \tau) y(\tau) d\tau \quad (16)$$

A numerical study of the actual experimental device (see Figure 2) which is illustrated in Figure 1 shows that when we use equidistant grids in space and time they are not well adapted. The time grid must be much more dense than that in space in order to obtain sufficient accuracy near the boundary $x = 0$. In Figure 1, the results of 3 computations with the same grid in space containing 20 points and 3 different grids in time, one with 20 points, another with 200 points and the last with 1000 points, are presented. The results show that 200 point grid is not sufficiently dense to get reasonably accurate results.

One possibility how to deal with the above problem (which is actually used in current simulation and experiments) is to use non-equidistant B-spline approximation with knot points which are more dense near time zero.

Another possibility is the following. The integral equation (16) describes the solution only in the interior ($0 < x < L$) of the spatial domain. Using the Fourier separation of variables technique and deriving from first principles we can obtain the following description of the solution for the whole spatial domain $0 \leq x \leq L$,

$$s(x, t) = y(t) + \int_{t_0}^t G_1(x, t - \tau) [-y(\tau) - by(\tau)] d\tau \quad (17)$$

where

$$\begin{aligned} G_1(x, t) &= \frac{4}{\pi} \sum_{n=0}^{\infty} \frac{1}{2n+1} \exp(-bt - \lambda_n t) \varphi_n(x) \\ &= \frac{4}{\pi} \sum_{n=0}^{\infty} \exp(-bt - \lambda_n t) \frac{\varphi_n(x)}{2n+1} \end{aligned} \quad (18)$$

The advantage of the kernel $G_1(x, t)$ is its better numerical behaviour. The series for this kernel converges faster and the grids are better adapted. However, the cost of this improvement is that the intuitive relation between the solution of the integral equation (16) and the function $y(t)$ is lost. As can be seen from (17), during the inverse problem solution there are two steps, firstly, the integral equation has to be solved and then the first order ordinary differential equation must be solved.

To see the relation between the system description (16) and (17), the equation (17) can be modified by integration by parts to give

$$\begin{aligned} s(x, t) &= y(t) - G_1(x, 0)y(t) + \\ &+ a^2 \int_{t_0}^t G_{\partial\xi}(x, t - \tau)y(\tau) d\tau \end{aligned} \quad (19)$$

This gives the same description inside the spatial domain as in (16) because for $0 < x \leq L$ $G_1(x, 0) = 1$. But for the point $x = 0$ the value $G_1(x, 0)$ is zero as well as the value of the integral kernel in (19) leading to the value $y(t)$ at the boundary.

4. Experimental results

The configuration of an experimental specimen on which the method has been verified is shown in Figure 2. It consists of a copper metal bar which is heated at one boundary and insulated at the other one. There are 8 thermocouples installed on the bar which can be used for the verification of the proposed method.

Equation (1) models the experimental device with a reasonable accuracy if the heat conduction and heat transfer coefficients are properly identified. We have used an off-line identification method, based on the fact that after reaching steady state of the system on some higher temperature we can switch the boundary condition at the heater side to the insulated-end Neumann type condition by simply switching off the heater. The system will relatively soon reach a state when the $\frac{\partial s}{\partial x}(x, t) \leq \epsilon_1$ for all $0 \leq x \leq L$ i.e. the temperature along the bar is nearly constant. ϵ_1 is an a-priori chosen small constant. In our case the system has been heated to the steady state with boundary temperature 260 degrees Celsius. Subsequently, after switching off the heater the system reached the state where ϵ_1 was under the level of the noise at about 60 degrees. From this moment the behaviour of the system is described by the simple first order differential equation $\frac{d}{dt}s + bs = 0$. This equation is solved analytically thus providing a possibility for high precision identification of the heat transfer coefficient. The

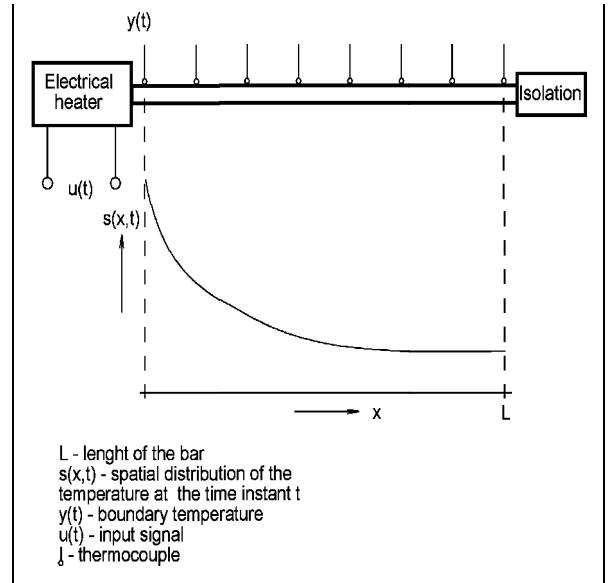


Figure 2: The experimental device consisting of a heater, a metal bar and a set of thermocouples. At the one end of the bar there is a heater. Another end is insulated. There are eight thermocouples along the bar. The main physical processes are the heat conduction from the heater and the heat transfer to the surrounding air. The power of the heater allows a temperature range 0-300 degrees Celsius.

results of this experiment are in Figure 3, where we use more and more points for computing b going backwards in time. Once we know accurately the heat transfer coefficient it is easy to compute the heat conduction coefficient by driving the system to steady state and solving the boundary problem for the first order ordinary differential equation. The resulting values are $b = 0.002$, $a = 0.0906$.

The experimental results are presented on the two sets of experiments. Both sets have the same structure but use the different values of the parameters a, b to illustrate the sensitivity of the proposed method to those parameter values.

Each set of the experiments is organized as follows: the experiment starts in a certain state of a system, then we submit subsequently in a step-wise manner 5 different states which the system must reach in an a-priori given time horizon. At the end of each time interval we compare the prescribed goal state with the state which the system has really reached and the internal simulation state which is maintained as a starting state for further steps of the step-wise method, as was described in detail in [12]. The actual measured state of the system is shown in 15 points but only every second one is obtained by direct measurement. The points between are interpolated by the use of splines.

The first set of experiments is given in Figure 4 and the second in Figure 5. In both sets, Figure A shows the boundary temperature. Figure B contains the heater controls and the remaining Figures t0-t5 show the states at the subsequent time steps.

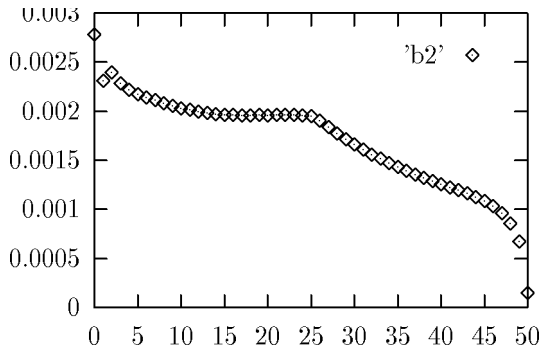


Figure 3: The identification of parameter b . The unit on the x-axis represents 100 seconds. The x-axis shows the computation of b in time going backwards

5. Conclusion

The experimental results support the developed step-wise method. However, during the verification process we have also identified certain drawbacks which show possible further research directions.

Some difficulties can be overcome by carefully choosing the spline representation base functions. Others are more inherent to the Green's function approach and could be overcome only by choosing a different approach. For example, when the equation is of a more complicated nature the explicit form of the Green's function could be not at hand. Also, during the forward problem solving the simulation with the integral kernels is rather computationally complex. Another problem is the reduced flexibility of the method due to the fixed time integration horizon, which asks for recalculation of the matrices each time the basic time step t_0 has to be changed.

One promising direction is the use of the well known numerically stable difference schemes, or finite elements, for the forward modelling. However, in this case the inverse problem formulation as well as numerical behaviour is a subject of current research.

6. Acknowledgement

The authors are grateful to the referees for very careful reading of the article and for suggesting improvements of the presentation.

References

- [1] Beck, J. V., Blackwell, B. and St. Clair, C. R., Jr., 1985, *Inverse Heat Conduction: Ill-Posed Problems*, (Wiley-Interscience, NY)
- [2] Butkovskiy, A.G., Structural theory of distributed parameter systems, *Elis Horwood Limited*, UK, (1983).
- [3] Curtain, R. F., Pritchard, A. J., 1978, Infinite dimensional linear systems theory, *Springer-Verlag, Berlin*.
- [4] Curtain, R. F., 1982, Finite-Dimensional Compensator Design for Parabolic Distributed Systems with Point Sensors and Boundary Input, *IEEE Transactions on Automatic Control*, Vol. AC-27, No.1, pp. 98-104.

- [5] Curtain, R. F., 1984, Finite Dimensional Compensators for Parabolic Distributed Systems with Unbounded Control and Observations, *SIAM J. Control and Optimization*, Vol. 22, No.2, pp. 255-276.
- [6] Glasko, V. B., Zacharov, A. V., Iljin, M. E., Noveshenko, J. A., Tichonov, A. N., 1984, O nekotorych zadachah optimizacii kvaziravnomernogo nagreva krupnogabaritnykh detalej, *Zhurnal vychislitelnoj matematiki i matematicheskoy fiziki*, Vol. 24, pp. 686-693.
- [7] Heath, M. T., 1974, *The Numerical Solution of Ill-Conditioned Systems of Linear Equations*, (Oak Ridge National Laboratory, Union Carbide Corporation)
- [8] Kárný, M., Nagy, I., Böhm, J., Halousková, A., Design of spline-based self-tuners, *Kybernetika*, Vol. 26, pp. 17-30, (1990).
- [9] Morozov, V. A., 1984, *Methods of Solving Incorrectly Posed Problems* (Springer-Verlag, New York)
- [10] Országhová, Z., Control of a class of distributed parameter systems based on model inversion. PhD thesis (in slovak), Slovak Technical University, Bratislava, (1993).
- [11] Powell, M.J.D., ZQPCVT a Fortran subroutine for convex quadratic programming. Report DAMTP/1983/NA17, Department of Applied Mathematics and Theoretical Physics, University of Cambridge, (1983).
- [12] Rohál-Ľkiv, B., Országhová, Z., and Hruz, T., 1993, A Stepwise Technique for Inverse Problem in Optimal Boundary Control of Thermal Systems, *Inverse Problems in Engineering, Theory and Practice, Proceedings of the First Conference in a Series on Inverse Problems in Engineering, Palm Coast, Florida* (Engineering Foundation by the American Society of Mechanical Engineers), pp. 147-153.
- [13] Rohál-Ľkiv, B., Zelinka, P., Spline-based predictive control: Introduction, *Spring school on: ADAPTIVE AND PREDICTIVE CONTROL*, Oxford, 21-22 March 1996.
- [14] Zelinka, P., Rohál-Ľkiv, B., Bencurik, B., Holicka, V., Spline-based predictive control: Practical experiments, *Spring school on: ADAPTIVE AND PREDICTIVE CONTROL*, Oxford, 21-22 March 1996.
- [15] Tarantola, A., 1987, *Inverse Problem Theory, Methods for Data Fitting and Model Parameter Estimation*, (Elsevier)
- [16] Tikhonov, A. N. and Arsenin, V. J., 1977, *Solution of Ill-Posed Problems* (V. H. Winston, Washington, D.C.)
- [17] Tikhonov, A. N. and Arsenin, V. J., 1979, *Metody reshenija nekorektnykh zadach, [Methods for Ill-Posed Problem Solving, in Russian]* (Nauka, Moscow)
- [18] Tikhonov, A. N., Goncsarskij, A. V., Stepanov, V. V. and Jagola, A. G., 1990, *Chislennyye metody reshenija nekorrektnykh zadach, [Numerical Methods for Ill-Posed Problem Solving, in Russian]* (Nauka, Moscow)
- [19] Widrow, B., 1987, Adaptive Inverse Control, in *2nd IFAC Workshop on Adaptive Systems in Control and Signal Processing, Sweden, Pergamon Press, Oxford*

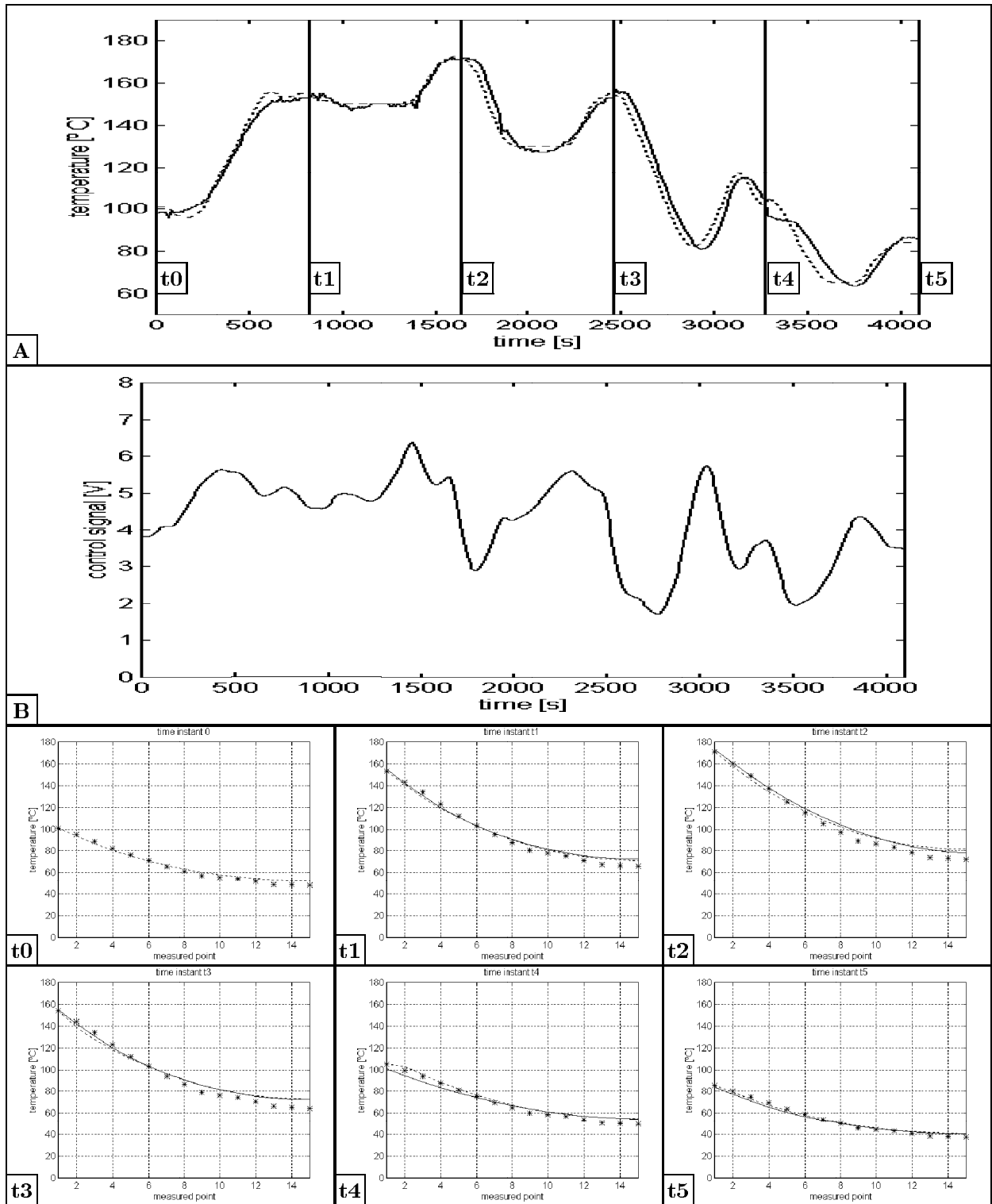


Figure 4: The set of experiments representing a continuous run of the system through goal states in step-wise way for the parameter values $a = 0.0906, b = 0.002$. In Figure A the full line shows the predicted temperature computed by solving the ill-posed inverse problem, the dashed line is the experimental temperature. In Figure B there is a control signal - the input to the heater. In the Figures t0-t5 there is a comparison of the prescribed goal state (full line) with the actually measured state (the stars) and the internal simulation state (dashed line) which is maintained as a starting state for further steps.

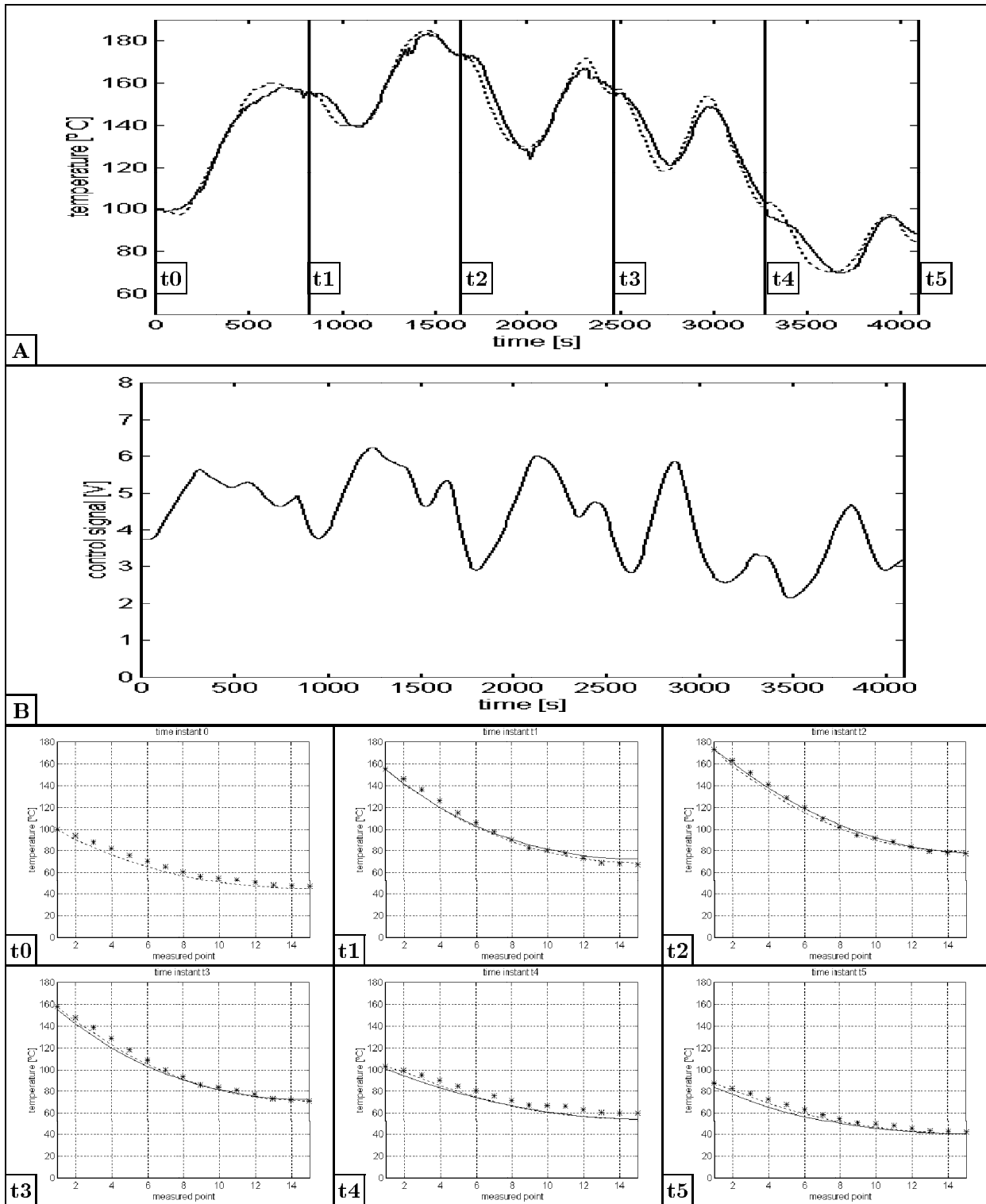


Figure 5: The set of experiments representing a continuous run of the system through goal states in step-wise way for the parameter values $a = 0.0135, b = 0.00485$. In Figure A the full line shows the predicted temperature computed by solving the ill-posed inverse problem, the dashed line is the experimental temperature. In Figure B there is a control signal - the input to the heater. In the Figures t_0 - t_5 there is a comparison of prescribed goal state (full line) with the actually measured state (the stars) and the internal simulation state (dashed line) which is maintained as a starting state for further steps.